

# Time-resolved and Superradiantly Amplified Unruh Signal

Akhil Deswal,<sup>1,\*</sup> Navdeep Arya,<sup>2,†</sup> Kinjalk Lochan,<sup>1,‡</sup> and Sandeep K. Goyal<sup>1,§</sup>

<sup>1</sup>*Department of Physical Sciences, Indian Institute of Science Education & Research (IISER) Mohali, Sector 81 SAS Nagar, Manauli PO 140306 Punjab India.*

<sup>2</sup>*Department of Physics, Stockholm University, Roslagstullsbacken 21, 106 91 Stockholm, Sweden*

An atom serves as a natural probe of quantum field fluctuations and any modifications to them, as fundamentally manifested in spontaneous emission. A collection of excited atoms can spontaneously develop correlations seeded by the vacuum fluctuations of the electromagnetic field. The correlations build over a finite time period, culminating in an intense, directional emission of photons known as superradiance. For a collection of atoms undergoing uniform linear acceleration, we identify low-acceleration conditions under which the buildup of correlations occurs faster and is driven solely by the modified field fluctuations underlying the Unruh effect — a prediction that a uniformly accelerated observer experiences the inertial vacuum as a thermal state. We demonstrate that these conditions can be realized inside a sub-resonant cavity that highly suppresses the response of an inertial atom, while still allowing significant response from an accelerated atom as, owing to the acceleration-induced spectral broadening, it can still couple to the available field modes. The field fluctuations perceived inertially under the sub-resonant cavity configuration would cause a superradiant burst much later. The early superradiant burst thus emerges as an unambiguous signature of the Unruh effect. In this way, we simultaneously address the extreme acceleration requirement, the weak signal, and the dominance of the inertial signal, all within a single experimental arrangement.

*Introduction*— The quantum field fluctuations are known to be altered under various conditions, leading to phenomena like the Casimir effect [1], the Schwinger effect [2], Hawking radiation [3], and particle creation in an expanding universe [4]. Additionally, the concepts of vacuum and particle content of a quantum field are inherently observer-dependent, as elegantly encapsulated in the Fulling-Davies-Unruh effect [5–8]—predicting that a uniformly accelerated observer perceives the inertial vacuum of a free quantum field to be in a thermal state at a temperature proportional to its acceleration.

While individual atoms provide valuable insights into such phenomena, a collection of atoms can function as an even more sophisticated probe [9], leveraging the rich dynamics of collective effects [10, 11]. For instance, photon emission from an extended sample of  $N$  excited atoms sensitively depends on the distribution of atoms in the sample and the properties of the electromagnetic field to which the atoms are coupled [12–15]. Although a single excited atom decays spontaneously with an exponential profile at an emission rate  $\gamma$ , the collective behavior of a group of atoms can significantly modify the emission process [10]. In an array of excited atoms where the atoms are indistinguishable with respect to their coupling to the electromagnetic field, correlations begin to develop between them as soon as any atom in the array undergoes spontaneous emission [11]. The correlations build up during a time period  $0 < \tau < \tau_d$ , ultimately leading to an intense event of photon emission, known as the superradiant burst, at the *superradiant delay time*  $\tau_d$ . The delay time is thus sensitive to the field fluctuations experienced by the atomic sample, and therefore should respond to, for example, the sample’s acceleration or the presence of a gravitational field [9]. The intense photon emission rate lasts for a short period  $\tau_{sr}$ , known as the

superradiance time. The superradiance process features a maximum emission rate scaling super-linearly with the total number of participating atoms, well-defined directionality, and a time-resolving nature characterized by the superradiant delay time  $\tau_d$  and the superradiance time  $\tau_{sr}$  [10, 11].

The Unruh effect, coveted partly due to its close connection to the Hawking effect [16], remains untested due to the requirement of extreme accelerations. At achievable accelerations, the expected signal, being extremely weak, will be overwhelmed by the inertial noise and the noise due to ambient laboratory temperature. The uniform acceleration induces non-resonant behavior in an atom, allowing it to couple to field modes in a broad frequency range. In this work, we leverage the acceleration-induced spectral broadening in combination with the hallmarks of superradiance to obtain a time-resolved and highly amplified Unruh signal at low accelerations.

To this end, we identify conditions under which the Unruh effect causes a faster buildup of correlations (due to higher emission rate) among the atoms while still preserving collective effects—leading to an early superradiant burst as its signature. A noticeable shift in  $\tau_d$  due to the Unruh effect is easier to isolate experimentally than a shift in an intensity amplitude only. Our ability to identify an experimental arrangement realizing the above-mentioned conditions depends on the observation that, in sharp contrast to an inertial atom, the acceleration-induced spectral broadening allows an accelerated atom to couple to the available field modes inside a sub-resonant cavity (an electromagnetic cavity formed by two parallel mirrors separated by a distance less than half of the transition wavelength of the atom). Under these conditions, the inertially perceived vacuum fluctuations would not suffice to build enough correlations for

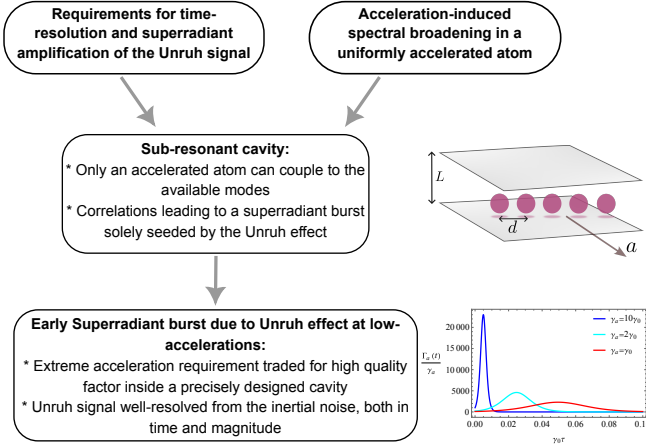


FIG. 1. Graphical summary of the results.

a superradiant burst in the given time. We thus address the problems of extreme acceleration requirement, weak signal, and the challenge of inertial noise (response due to field fluctuations perceived inertially) in a single setup. Refer to Fig. 1 for a graphical summary of the results.

*Collective response of atoms*— Consider an ensemble of  $N$  identical two-level atoms taking positions  $\mathbf{r}_i$ , coupled to a real massless quantum scalar field  $\hat{\Phi}(\tau, \mathbf{r}_i)$  between two parallel mirrors with separation  $L$ , and complex reflection and transmission coefficients  $r$  and  $t$ , respectively. Each atom carries a monopole moment  $\hat{\mathbf{m}}_j = i(\hat{\sigma}_j^- - \hat{\sigma}_j^+)$ , where  $\hat{\sigma}_j^\pm$  are the atomic raising and lowering operators for the  $j$ th atom. The free Hamiltonian of each atom is  $\hat{H}_j = \omega_0 \hat{\sigma}_j^z / 2$ , where  $\hat{\sigma}_j^z$  is the Pauli  $z$ -matrix for the  $j$ th atom and  $\omega_0$  is the transition frequency. The corresponding transition wavelength is denoted by  $\lambda_0$ . The atom-field interaction Hamiltonian, in the comoving frame of the atoms,  $\hat{H}_I = \sum_{i=1}^N \hat{\mathbf{m}}_i(\tau) \otimes \hat{\Phi}(\tau, \mathbf{r}_i)$ , corresponds to the atom-light interaction in the dipole-approximation, simplified to describe interaction between an atom and a single polarization of the electromagnetic field [17–19]. We take the atoms to form a one-dimensional ordered array with interatomic spacing  $d\hat{y}$  transverse to its motion. Hereafter, we address an array subjected to uniform linear acceleration, in which each atom takes the trajectory  $t(\tau) = a^{-1} \sinh(a\tau)$ ,  $z(\tau) = a^{-1} \cosh(a\tau)$ , as a Rindler array. Here,  $\tau$  is the proper time of the atom.

The total emission rate of a Rindler array is obtained as (see appendix)

$$\Gamma_a(\tau) = \frac{\gamma_a}{4\mu_a} (\mu_a N + 1)^2 \operatorname{sech}^2 \left( \frac{\tau - \tau_d}{2\tau_{\text{sr}}} \right), \quad (1)$$

where  $\gamma_a$  is the emission rate of a single Rindler atom,  $\tau_d = \ln(\mu_a N) / \gamma_a (\mu_a N + 1)$  is the superradiant delay time, and  $\tau_{\text{sr}} = 1 / \gamma_a (\mu_a N + 1)$  is the superradiance time as marked in Fig. 2(c). The *shape factor*  $\mu_a$  of the accel-

ated array is defined as  $\mu_a \equiv \gamma_a^{-1} N^{-2} \sum_{i \neq j} \gamma_{ij}^{(a)}$ , where

$$\gamma_{ij}^{(a)} = 2 \int \frac{d^2 k_\perp}{(2\pi)^3} \int_0^\infty d\omega'_k \Theta(\omega'_k - k_\perp) \frac{\rho(k_x, L, \mathcal{R})}{\sqrt{\omega_k'^2 - k_\perp^2}} \times e^{ik_y \Delta y_{ij}} \int_{-\infty}^\infty ds e^{i\omega_0 s} \exp \left( -\frac{2i\omega'_k}{a} \sinh \left( \frac{as}{2} \right) \right), \quad (2)$$

for  $i \neq j$ , quantifies the extent to which  $i$ th and  $j$ th atoms in the array influence each other's dynamics,  $k_\perp \equiv \sqrt{k_x^2 + k_y^2}$ ,  $\Theta(x)$  is the Heaviside theta function,  $\Delta y_{ij} \equiv y_i - y_j$ ,  $s \equiv \tau_i - \tau_j$ ,  $\omega'_k = \omega_k \cosh(a\tau) - k_z \sinh(a\tau)$ ,  $k'_z = k_z \cosh(a\tau) - \omega_k \sinh(a\tau)$ , and

$$\rho(k_x, L, \mathcal{R}) \equiv \frac{(1 + \mathcal{R}^2) - 2\mathcal{R} \cos(k_x L)}{(1 - \mathcal{R}^2) + \frac{4\mathcal{R}^2 \sin^2(k_x L)}{(1 - \mathcal{R}^2)}}, \quad (3)$$

is the density of field modes as modified by the planar cavity formed by two parallel mirrors having reflectivity  $\mathcal{R}$ .

The shape factor contains information about the distribution of atoms in the sample and the properties, like mode structure and particle content, of the field to which the atoms are coupled. In addition, it is sensitive to the state of motion of the array and the presence of any gravitational effects [9]. In particular, note that the ‘‘cooperation’’  $\gamma_{ij}^{(a)}$  between  $i$ th and  $j$ th atoms in the array depends on the array's acceleration.

*Condition for time-resolution and superradiant enhancement*— An intuitive way to appreciate the shape factor is to think of  $\mu N$  as the effective number of cooperating atoms [13]. In the small sample limit, the so-called Dicke regime [10],  $\mu N \rightarrow N - 1$ , meaning that all the atoms in the sample cooperate, that is, the cooperative effects are strong. In general, under the effect of uniform acceleration,  $\gamma_a / \gamma_0 \equiv \zeta$  increases while  $\mu_a N / \mu_0 N \equiv \chi$  decreases as a function of acceleration (see Fig. 2(b)). We are interested in resolving the superradiant burst of a Rindler array from that of an inertial array. The occurrence of the two superradiant peaks will differ if the corresponding superradiant delay times are different enough. Further, the overlap of the two superradiant temporal profiles can be reduced if the collective effects are not compromised much due to the acceleration—this ensures that  $\tau_{\text{sr}}$ , the time period over which superradiance occurs, remains small.

To this end, consider the ratio of the superradiant delay times for a Rindler and an inertial array:

$$\frac{\tau_d^{(a)}}{\tau_d^{(0)}} = \frac{\gamma_0 (\mu_0 N + 1) \ln(\mu_a N)}{\gamma_a (\mu_a N + 1) \ln(\mu_0 N)}. \quad (4)$$

The two signals are well-resolved in time if  $\tau_d^{(a)} \ll \tau_d^{(0)}$ . If we chose  $d/\lambda_0$  such that both  $\mu_a N$  and  $\mu_0 N$  are much greater than 1 (ensuring strong collective effects), the

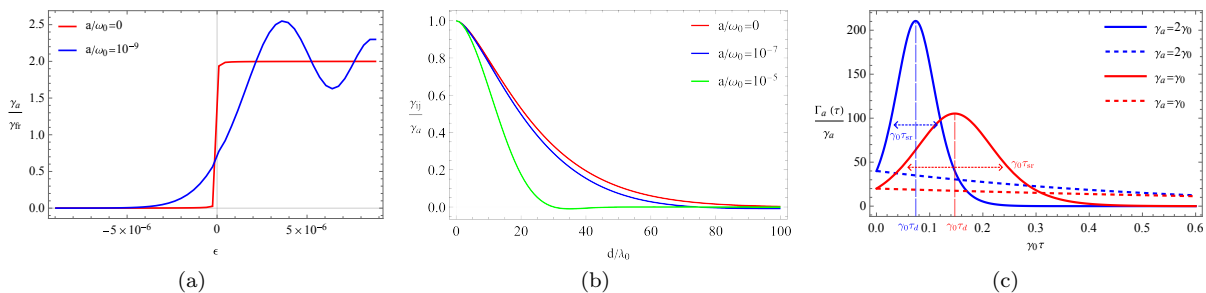


FIG. 2. **Interplay of acceleration-induced spectral broadening and collective effects inside a sub-resonant cavity.**

(a) Behavior of the emission rate of an inertial and a Rindler atom as a function of the cavity detuning parameter  $\epsilon$  (defined as  $\omega_0 L = \pi - \epsilon$ ), for  $\mathcal{R} = 1 - 10^{-8}$ . Here,  $\gamma_{fr}$  is the spontaneous emission rate of a single inertial atom in free space. For  $\epsilon < 0$ , that is  $L < \lambda_0/2$ , the emission rate of an inertial atom is highly suppressed, whereas the emission rate of a Rindler atom falls to the same extent for much lower mirror separation. (b) Impact of acceleration on  $\gamma_{ij}^{(a)}/\gamma_a$ , the cooperation between  $i$ th and  $j$ th atoms, as a function of separation between the two atoms inside a sub-resonant cavity with  $\mathcal{R} = 1 - 10^{-4}$ . For a given separation between the two atoms, cooperation between them diminishes for increasing acceleration. The ‘‘cooperation’’ quantifies the extent to which an atom influences the emission process of another atom. (c) Comparison of the temporal behavior of the emission rate of an incoherent sample (dashed curves) of atoms versus that of a superradiant sample (solid curves). The temporal emission profile of inertial and Rindler samples of independent atoms overlap with each other. In superradiant samples however, the two signals can be resolved as the superradiance process has a time-resolving nature characterized by the delay time  $\tau_d$  and the superradiance time  $\tau_{sr}$ . We leverage the collective response of an array of atoms inside a sub-resonant cavity to obtain a time-resolved and superradiantly amplified Unruh signal.

requirement simplifies to

$$\frac{\tau_d^{(a)}}{\tau_d^{(0)}} \approx \frac{\gamma_0 \mu_0 N \ln(\mu_a N)}{\gamma_a \mu_a N \ln(\mu_0 N)} \ll 1. \quad (5)$$

At the same time, since the maximum superradiant emission rate scales as  $(\mu N)^2$ , if we want time-resolution of the two signals without compromising on superradiant amplification of the noninertial signal, we additionally require  $\mu_a/\mu_0 \approx 1$  (with  $\mu_a$  and  $\mu_0$  each individually close to unity). Thus, the requirements to *time-resolve and superradiantly amplify* the Unruh signal are  $\gamma_a/\gamma_0 \gg 1$  and  $\mu_a/\mu_0 \approx 1$ . Under these conditions, the correlations between atoms that eventually lead to a superradiant burst build much faster in a Rindler array, with the buildup exclusively driven by the Unruh effect. The superradiant burst would thus be solely seeded by the modified field fluctuations underlying the Unruh effect predicted to be experienced by an accelerated system. This early superradiant burst would serve as a clear signature of the Unruh effect.

To understand the effect of acceleration on  $\mu$ , in Fig. 2(b) we analyze the behavior of  $\gamma_{ij}^{(a)}/\gamma_a$  as a function of  $d/\lambda_0$  for different accelerations. Note that for a larger acceleration ( $a/\omega_0 \sim 10^{-5}$ ), the cooperation between  $i$ th and  $j$ th atoms is quickly reduced with increasing  $d/\lambda_0$ . On the other hand, for a smaller acceleration ( $a/\omega_0 \sim 10^{-7}$ ), the cooperation is almost the same as for the inertial case over the range of  $d/\lambda_0$  shown. Therefore, larger the acceleration, quicker is the fall in  $\gamma_{ij}^{(a)}/\gamma_a$  with increasing  $d/\lambda_0$ . Importantly, a finite, yet small, interatomic distance is required to preserve collective effects

against dephasing due to coherent dipole-dipole interactions [11]. This effect in our setup is analyzed in the appendix.

Therefore, the requirement of  $\mu_a/\mu_0 \approx 1$  is comfortably fulfilled at low accelerations. Next, note that in general the emission rate  $\gamma_a$  of an accelerated atom can be written as  $\gamma_a = \gamma_0 + \tilde{\gamma}(\alpha)$ ,  $\alpha \equiv a/\omega_0$ , where the last contribution is purely-noninertial, that is,  $\lim_{\alpha \rightarrow 0} \tilde{\gamma}(\alpha) = 0$ . As we have already noted that  $\mu_a/\mu_0 \approx 1$  can be achieved at low accelerations, clearly, the time-resolution and superradiant enhancement of the Unruh signal hinges on achieving  $\gamma_a/\gamma_0 \gg 1$ . For  $\gamma_a/\gamma_0 = 1 + \tilde{\gamma}/\gamma_0$  to be much greater than unity, we require  $\tilde{\gamma}/\gamma_0 \gg 1$ , which could not be achieved in any of the proposals for observing the Unruh effect so far.

Next, we demonstrate that  $\tilde{\gamma}(\alpha)/\gamma_0 \gg 1$  can be achieved inside a sub-resonant cavity by optimally harnessing the acceleration-induced non-resonant behavior of a Rindler atom.

*Acceleration-induced spectral broadening*— The Eq. (2) can be cast in a more general form as  $\gamma_{ij}^{(a)} \propto \int_0^\infty d\omega'_k \rho(\omega'_k) e^{ik_y \Delta y_{ij}} \mathcal{I}(\omega'_k, \omega_0, a)$ , where  $\rho(\omega'_k)$  is the density of field modes and  $\mathcal{I}(\omega'_k, \omega_0, a)$  decides the field modes participating in the atomic system’s response. The uniform acceleration induces non-resonant behavior in an atom, causing spectral broadening [20, 21]. The emission rate of a single inertial ( $a = 0$ ) and Rindler ( $a \neq 0$ ) atom can be obtained by setting  $i = j$  in Eq. (2). The difference,  $\gamma_a - \gamma_0$ , in the two responses hinges on the Rindler atom perceiving the Minkowski plane waves with a time-dependent phase as is evident in the  $\exp(-2i(\omega'_k/a) \sinh(as/2))$  factor, as opposed to

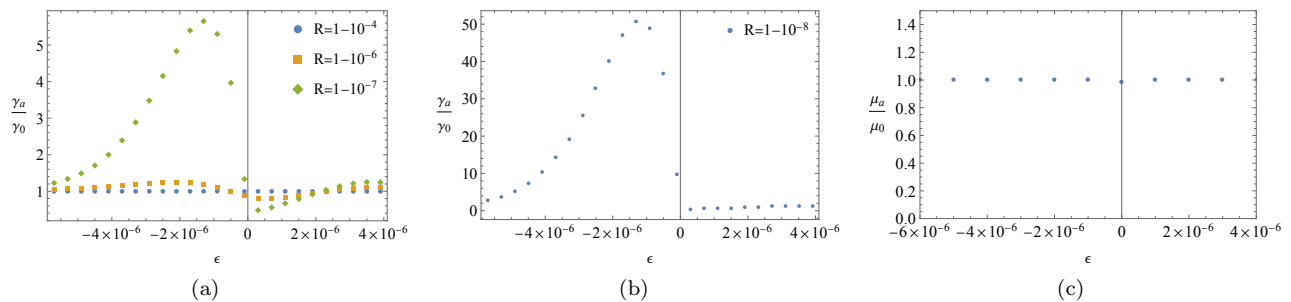


FIG. 3. **Realization of conditions for time-resolution and superradiant enhancement of the Unruh signal inside a sub-resonant cavity.** (a),(b) Dependence of  $\gamma_a/\gamma_0$  on the reflectivity (equivalently, quality factor) and the cavity detuning parameter  $\epsilon$ . Inside a sub-resonant cavity, higher mirror reflectivity leads to higher  $\gamma_a/\gamma_0$  values due to a stronger suppression of the emission rate of an inertial atom, while a Rindler atom still responds significantly due to the acceleration-induced non-resonant behavior. As  $\gamma_a/\gamma_0 = 1 + \tilde{\gamma}(\alpha)/\gamma_0$ , unambiguously resolving the purely-noninertial signal  $\tilde{\gamma}(\alpha)$  against the inertial signal  $\gamma_0$  requires  $\tilde{\gamma}(\alpha)/\gamma_0 \geq 1$ , that is,  $\gamma_a/\gamma_0 \geq 2$ . For  $\alpha \equiv a/\omega_0 = 10^{-9}$ , the two signals are not resolved unless the mirror reflectivity is equal to or better than  $1 - 10^{-7}$ , for which the two signals are well-resolved in a sub-resonant cavity configuration. In (b), the required precision in the specification of cavity width to access  $\gamma_a/\gamma_0 \gg 1$  is  $\Delta L/L \sim 10^{-6}$ . (c) The ratio  $\mu_a/\mu_0$  of the Rindler and inertial shape factors, for an atom array with  $d/\lambda_0 = 1$ , remains nearly constant over the cavity detuning range of interest. For all the plots,  $a/\omega_0 = 10^{-9}$ .

a factor of  $\exp(-i\omega_k s)$  for an inertial atom (note that  $\lim_{a \rightarrow 0} \exp(-2i(\omega'_k/a) \sinh(as/2)) = \exp(-i\omega_k s)$ ).

In the case of an inertial atom,  $\mathcal{I}_{\text{inertial}} \equiv \int_{-\infty}^{+\infty} ds e^{i\omega_0 s} e^{-i\omega_k s} = 2\pi\delta(\omega_k - \omega_0)$  enforces resonant coupling of the atom to field modes with frequency  $\omega_0$ . In sharp contrast, however, for a Rindler atom, the time integral doesn't lead to a Dirac delta function:

$$\begin{aligned} \mathcal{I}_{\text{Rindler}} &\equiv \int_{-\infty}^{+\infty} ds e^{i\omega_0 s} e^{-2i(\omega'_k/a) \sinh(as/2)} \\ &= \frac{4}{a} e^{\pi\omega_0/a} K_{2i\omega_0/a} \left( \frac{2\omega_0 \omega'_k}{a \omega_0} \right), \end{aligned} \quad (6)$$

where  $K_\nu(x)$  is the modified Bessel function of the second kind. Note that  $\mathcal{I}_{\text{Rindler}}$  doesn't strictly enforce  $\omega'_k/\omega_0 = 1$ , unless  $a \rightarrow 0$ , as illustrated in Fig. 4. Thus, acceleration induces a non-resonant behavior in the atom, broadening its spectrum. In Fig. 4, we note some intriguing features in a Rindler atom's coupling to field modes: for  $\omega'_k < \omega_0$ , the atom couples constructively to some field modes and destructively to others. Moreover, it couples (constructively) to modes having  $\omega'_k > \omega_0$ . An atom placed inside a sub-resonant cavity experiences such a condition where all the available field modes have frequency greater than the atom's transition frequency. Earlier proposals [21–23] using density of field modes to relax acceleration requirement did not fully exploit the acceleration-induced spectral broadening as they focused on cavities tuned above the first resonance point, limiting the signal-to-noise ratio ( $\tilde{\gamma}/\gamma_0 \lesssim 1$ ) that could be achieved in such setups, as analyzed in Figs. 3(a),3(b). Next, we analyze acceleration-induced spectral broadening inside a sub-resonant cavity.

*Effect of mirror separation*— The spontaneous emission rate of a single inertial atom placed between two

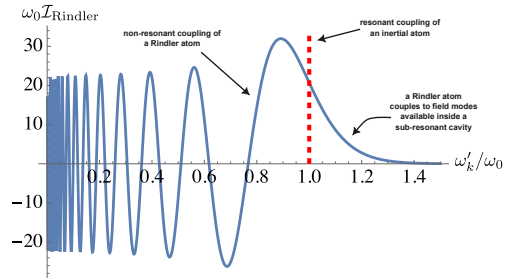


FIG. 4. **Acceleration-induced spectral broadening in a Rindler atom.** The red dashed line shows an inertial atom's resonant coupling, i.e., to modes with  $\omega'_k \approx \omega_0$ . The blue curve shows non-resonant coupling of a Rindler atom to field modes. In particular, note a Rindler atom's coupling to field modes with  $\omega'_k > \omega_0$ , a feature that can be optimally exploited inside a sub-resonant cavity. The plot is for  $a/\omega_0 = 10^{-1}$ .

perfect mirrors is obtained by taking  $\mathcal{R} \rightarrow 1$ ,  $a \rightarrow 0$ , and  $i = j$  in Eq. (2):

$$\gamma_0 = \frac{1}{L} \sum_{n=1}^{\infty} \sin^2\left(\frac{n\pi}{2}\right) \Theta\left(1 - \frac{n\lambda_0}{2L}\right). \quad (7)$$

Note that  $\gamma_0$  receives contributions from field modes with  $n < 2L/\lambda_0$ . In particular, if the separation between the mirrors is less than  $\lambda_0/2$ , there are no field modes available to facilitate spontaneous emission from the atom, leading to a vanishing  $\gamma_0$  [24–26]. However, any realistic mirrors would have a reflectivity less than unity and therefore the emission rate for  $L < \lambda_0/2$  decreases smoothly with decreasing  $L$  (see Fig. A2).

On the other hand, due to acceleration-induced non-resonant behavior, a Rindler atom shows a stronger emission rate as the mirror separation is lowered below the

first resonance point. Figure 2(a) compares the emission rates of an inertial and Rindler atom as a function of mirror separation and clearly shows a stronger emission rate of the Rindler atom below the first resonance point. As a result, in the sub-resonant configuration of the cavity, a large  $\gamma_a/\gamma_0$  ratio can be obtained. However, note that the emission rate for even an accelerated single atom in this cavity configuration is extremely weak. But, with many cooperatively behaving atoms ( $\mu_a N \approx \mu_0 N \gg 1$ ), which is possible at low accelerations with  $d/\lambda_0$  lying in an appropriate range, the two rates can be superradiantly amplified for an array of atoms. In flat spacetime, smaller interatomic spacing generally enhances the collective emission rate, provided that dephasing caused by coherent dipole-dipole interactions does not suppress the collective behavior [11]. The detrimental effects of these interactions can be mitigated by arranging the atoms in an ordered array [27, 28]. For that reason, we have considered an ordered array of atoms (see appendix for more details).

In Figs. 3(a) and 3(b), we plot the ratio  $\gamma_a/\gamma_0$  as a function of mirror separation for different values of mirror reflectivity. For the reflectivities  $\mathcal{R} < 1$ , mirror separations  $L > \lambda_0/2$  lead to  $\gamma_a/\gamma_0 \sim 1$ , that is,  $\tilde{\gamma}/\gamma_0 \ll 1$ . However, for mirror separations  $L < \lambda_0/2$  and for a given acceleration of the Rindler atom, the ratio  $\gamma_a/\gamma_0$  increases with higher mirror reflectivities, taking values as large as 50 for  $\mathcal{R} = 1 - 10^{-8}$ ,  $a \sim 10^{-9}\omega_0 c$  (where we have momentarily restored  $c$ ). Thus, the sub-resonant cavity configuration achieves  $\tilde{\gamma}(\alpha)/\gamma_0 \gg 1$ , as required. Moreover, in the same parameter range,  $\mu_a/\mu_0 \approx 1$  as shown in Fig. 3(c).

To summarize, combined with  $\mu N \gg 1$ , these conditions mean that the buildup of correlations among atoms required for a superradiant burst, occurs faster in a Rindler array and is driven dominantly by the Unruh effect as  $\tilde{\gamma}(\alpha)/\gamma_0 \gg 1$ . The field fluctuations perceived inertially under these conditions will be entirely inadequate to cause a superradiant burst in the given time. The early superradiant burst is thus entirely seeded by the modified field fluctuations underlying the Unruh effect experienced by the accelerated array of atoms—giving us a time-resolved and superradiantly amplified Unruh signal.

*Implementation*— The requirement of acceleration and the recent demonstration of robustness of collective effects in relatively noisy conditions in NV centers in a diamond membrane coupled to a high-finesse cavity [29] suggest that such solid-state platforms can be used to test for the early superradiant burst caused by the Unruh effect. The idea of *time-resolution accompanying superradiant amplification* can be first tested in compact prototype experiments subjecting a collection of atoms to non-linear accelerations [30–34], and potentially in analog systems [35–37]. In all these scenarios, the modified stronger field fluctuations experienced by the accelerated

$\alpha = a/\omega_0 c$	$ \mathcal{R}_{\min} $	$\omega_0 L/c = 2\pi L/\lambda_0$	$Q_{\min}$
$10^{-11}$	$1 - 10^{-9}$	$\pi - 10^{-8}$	$\pi \times 10^9$
$10^{-10}$	$1 - 10^{-8}$	$\pi - 10^{-7}$	$\pi \times 10^8$
$10^{-9}$	$1 - 10^{-7}$	$\pi - 10^{-6}$	$\pi \times 10^7$

TABLE I. **Requirement of extreme accelerations can be traded for high quality factor inside a precisely designed cavity.** Minimum required quality factor,  $Q_{\min} = 2\pi L/\lambda_0(1 - |\mathcal{R}_{\min}|)$ , of the cavity mirrors to resolve the non-inertial signal for various values of  $\alpha$ . The Unruh signal can be resolved from the inertial signal at lower accelerations inside a precisely designed cavity if the cavity mirrors have a correspondingly higher quality factor.

sample should lead to an early superradiant burst under appropriate conditions.

*Conclusion*— We have addressed three key challenges facing any potential experimental enterprise to observe the Unruh effect. The requirement of extreme acceleration can be traded for high quality factor inside a precisely designed cavity. By identifying conditions under which a superradiant burst is exclusively seeded by the Unruh effect, we demonstrated a highly amplified and temporally resolved Unruh signal relative to the inertial signal, inside a sub-resonant cavity. A clear separation in time between the Unruh and the inertial signals addresses the challenge of inertial noise overwhelming the purely-noninertial signal. The sub-resonant cavity setup is inspired by the acceleration-induced non-resonant behavior of the Rindler atom that allows it to respond even when all available field modes have a higher frequency than its transition frequency. An inertial atom’s response is highly suppressed in this cavity configuration. We thus identify laboratory conditions and tools that magnify the subtle observer-dependent field theoretic effects to a detectable level. Finally, the equivalence principle points to the gravitational analogues of the effects presented here—gravity-induced spectral broadening of atoms, and a collective quantum response seeded by gravity [9].

*Acknowledgments*— A.D. acknowledges funding from IISER Mohali. N.A. thanks Jorma Louko, Jerzy Paczos, and Magdalena Zych for helpful discussions and useful comments. N.A. acknowledges funding from Knut and Alice Wallenberg foundation through a Wallenberg Academy Fellowship No. 2021.0119. Research of K.L. is partially supported by SERB, Government of India, through a MATRICS research grant no. MTR/2022/000900.

*Author Contributions*— N.A. and A.D. conceptualized the research. A.D. and N.A. performed the formal

analysis and investigation. All the authors contributed to the interpretation and validation of the results and to the manuscript writing.

---

\* akhildeswal.phy@gmail.com

† navdeeparya.me@gmail.com; navdeep.arya@fysik.su.se

‡ kinjalk@iisermohali.ac.in

§ skgoyal@iisermohali.ac.in

- [1] H. B. G. Casimir and D. Polder, The influence of retardation on the london-van der waals forces, *Phys. Rev.* **73**, 360 (1948).
- [2] J. Schwinger, On gauge invariance and vacuum polarization, *Phys. Rev.* **82**, 664 (1951).
- [3] S. W. Hawking, Black hole explosions?, *Nature* **248**, 30 (1974).
- [4] L. Parker, Particle creation in expanding universes, *Phys. Rev. Lett.* **21**, 562 (1968).
- [5] S. A. Fulling, Nonuniqueness of canonical field quantization in Riemannian space-time, *Phys. Rev. D* **7**, 2850 (1973).
- [6] P. C. W. Davies, Scalar production in Schwarzschild and Rindlermetrics, *Journal of Physics A: Mathematical and General* **8**, 609 (1975).
- [7] W. G. Unruh, Notes on black-hole evaporation, *Phys. Rev. D* **14**, 870 (1976).
- [8] C. A. U. Lima, F. Brito, J. Hoyos, and D. A. T. Vanzella, Probing the Unruh effect with an accelerated extended system, *Nature Communications* **10**, 3030 (2019).
- [9] N. Arya and M. Zych, Selective amplification of a gravitational wave signal using an atomic array, arXiv preprint arXiv:2408.12436 10.48550/arXiv.2408.12436 (2024).
- [10] R. H. Dicke, Coherence in spontaneous radiation processes, *Phys. Rev.* **93**, 99 (1954).
- [11] M. Gross and S. Haroche, Superradiance: An essay on the theory of collective spontaneous emission, *Physics Reports* **93**, 301 (1982).
- [12] J. Eberly and N. Rehler, Dynamics of superradiant emission, *Physics Letters A* **29**, 142 (1969).
- [13] N. E. Rehler and J. H. Eberly, Superradiance, *Phys. Rev. A* **3**, 1735 (1971).
- [14] J. H. Eberly, Superradiance Revisited, *American Journal of Physics* **40**, 1374 (1972).
- [15] G. S. Agarwal, Master-equation approach to spontaneous emission, *Phys. Rev. A* **2**, 2038 (1970).
- [16] V. Mukhanov and S. Winitzki, *Introduction to Quantum Effects in Gravity* (Cambridge University Press, 2007).
- [17] B. Šoda, V. Sudhir, and A. Kempf, Acceleration-induced effects in stimulated light-matter interactions, *Phys. Rev. Lett.* **128**, 163603 (2022).
- [18] E. Martín-Martínez, M. Montero, and M. del Rey, Wavepacket detection with the Unruh-DeWitt model, *Phys. Rev. D* **87**, 064038 (2013).
- [19] A. M. Alhambra, A. Kempf, and E. Martín-Martínez, Casimir forces on atoms in optical cavities, *Phys. Rev. A* **89**, 033835 (2014).
- [20] P. M. Alsing and P. W. Milonni, Simplified derivation of the Hawking-Unruh temperature for an accelerated observer in vacuum, *American Journal of Physics* **72**, 1524 (2004).
- [21] D. J. Stargen and K. Lochan, Cavity optimization for Unruh effect at small accelerations, *Phys. Rev. Lett.* **129**, 111303 (2022).
- [22] N. Arya, D. J. Stargen, K. Lochan, and S. K. Goyal, Strong noninertial radiative shifts in atomic spectra at low accelerations, *Phys. Rev. D* **110**, 085007 (2024).
- [23] D. Barman, D. Ghosh, and B. R. Majhi, Mirror-enhanced acceleration induced geometric phase: towards detection of Unruh effect (2024), arXiv:2405.07711 [quant-ph].
- [24] D. J. Heinzen and M. S. Feld, Vacuum radiative level shift and spontaneous-emission linewidth of an atom in an optical resonator, *Phys. Rev. Lett.* **59**, 2623 (1987).
- [25] F. D. Martini, G. Innocenti, G. R. Jacobovitz, and P. Mataloni, Anomalous spontaneous emission time in a microscopic optical cavity, *Phys. Rev. Lett.* **59**, 2955 (1987).
- [26] W. Jhe, A. Anderson, E. A. Hinds, D. Meschede, L. Moi, and S. Haroche, Suppression of spontaneous decay at optical frequencies: Test of vacuum-field anisotropy in confined space, *Phys. Rev. Lett.* **58**, 666 (1987).
- [27] S. J. Masson, I. Ferrier-Barbut, L. A. Orozco, A. Browaeys, and A. Asenjo-Garcia, Many-body signatures of collective decay in atomic chains, *Phys. Rev. Lett.* **125**, 263601 (2020).
- [28] S. J. Masson and A. Asenjo-Garcia, Universality of Dicke superradiance in arrays of quantum emitters, *Nature Communications* **13**, 2285 (2022).
- [29] M. Pallmann, K. Köster, Y. Zhang, J. Heupel, T. Eichhorn, C. Popov, K. Mølmer, and D. Hunger, Cavity-mediated collective emission from few emitters in a diamond membrane, *Phys. Rev. X* **14**, 041055 (2024).
- [30] K. Lochan, H. Ulbricht, A. Vinante, and S. K. Goyal, Detecting Acceleration-Enhanced Vacuum Fluctuations with Atoms Inside a Cavity, *Phys. Rev. Lett.* **125**, 241301 (2020), arXiv:1909.09396 [gr-qc].
- [31] H. Wang and M. Blencowe, Coherently amplifying photon production from vacuum with a dense cloud of accelerating photodetectors, *Communications Physics* **4**, 128 (2021).
- [32] N. Arya, V. Mittal, K. Lochan, and S. K. Goyal, Geometric phase assisted observation of noninertial cavity-QED effects, *Phys. Rev. D* **106**, 045011 (2022).
- [33] N. Arya and S. K. Goyal, Lamb shift as a witness for quantum noninertial effects, *Phys. Rev. D* **108**, 085011 (2023).
- [34] H.-T. Zheng, X.-F. Zhou, G.-C. Guo, and Z.-W. Zhou, Enhancing analog unruh effect via superradiance in a cylindrical cavity, *Phys. Rev. Res.* **7**, 013027 (2025).
- [35] P. M. Alsing, J. P. Dowling, and G. J. Milburn, Ion trap simulations of quantum fields in an expanding universe, *Phys. Rev. Lett.* **94**, 220401 (2005).
- [36] C. Gooding, S. Biermann, S. Erne, J. Louko, W. G. Unruh, J. Schmiedmayer, and S. Weinfurter, Interferometric Unruh detectors for Bose-Einstein condensates, *Phys. Rev. Lett.* **125**, 213603 (2020).
- [37] Z. Tian, X. Cheng, Y. Li, X. Zhao, W. Hou, M. Zhu, L. Yan, K. Rehan, X. Qin, Y. Lin, *et al.*, Quantum simulation of oscillatory Unruh effect with superposed trajectories, Preprint 10.21203/rs.3.rs-4753072/v1 (2024).
- [38] H.-P. Breuer and F. Petruccione, *The theory of open quantum systems* (Oxford University Press on Demand, 2002).
- [39] F. De Martini, M. Marrocco, P. Mataloni, L. Crescentini, and R. Loudon, Spontaneous emission in the optical

microscopic cavity, *Phys. Rev. A* **43**, 2480 (1991).

- [40] M. Ley and R. Loudon, Quantum theory of high-resolution length measurement with a fabry-perot interferometer, *Journal of Modern Optics* **34**, 227 (1987).
- [41] R. Friedberg, S. Hartmann, and J. Manassah, Frequency shifts in emission and absorption by resonant systems of two-level atoms, *Physics Reports* **7**, 101 (1973).
- [42] G. S. Agarwal, Master-equation approach to spontaneous emission. III. many-body aspects of emission from two-level atoms and the effect of inhomogeneous broadening, *Phys. Rev. A* **4**, 1791 (1971).

## APPENDIX

### Superradiant Master Equation

The Lindblad master equation governing the dynamics of the atomic array is given as [11]

$$\frac{d\hat{\rho}(\tau)}{d\tau} = -i[\hat{H}_{\text{eff}}, \hat{\rho}(\tau)] + \sum_{i,j} \gamma_{ij} \left( \hat{\sigma}_j^- \hat{\rho}(\tau) \hat{\sigma}_i^+ - \frac{1}{2} \{ \hat{\sigma}_i^+ \hat{\sigma}_j^-, \hat{\rho}(\tau) \} \right), \quad (\text{A1})$$

where  $\hat{\rho}(\tau)$  is the reduced atomic density operator and  $\tau$  is the proper time. The first term on the right hand side of the above equation drives Hamiltonian evolution of the system with [11, 38]

$$\hat{H}_{\text{eff}} = \sum_{i,j} \Omega_{ij} \hat{\sigma}_i^+ \hat{\sigma}_j^-, \quad (\text{A2})$$

where  $\Omega_{ij} = \text{Im}\{\Gamma_{ij}(\omega_0) + \Gamma_{ij}(-\omega_0)\}$ ,  $\Gamma_{ij}(\omega) = \int_0^\infty d\tau e^{i\omega\tau} \langle \hat{\Phi}(\tilde{x}_i(\tau)) \hat{\Phi}(\tilde{x}_j(0)) \rangle$ , and  $\tilde{x}$  denotes a spacetime event. The second term in Eq. (A1) controls the dissipative dynamics of the atoms, where  $\gamma_{ij}$  is the Fourier transform of the two-point field correlation function:

$$\gamma_{ij}(\omega) = \int_{-\infty}^{\infty} d\tau e^{i\omega\tau} \langle \hat{\Phi}(\tilde{x}_i(\tau)) \hat{\Phi}(\tilde{x}_j(0)) \rangle. \quad (\text{A3})$$

From Eq. (A1), the total emission rate of the array is obtained as:

$$\Gamma(\tau) = \sum_{i=1}^N \gamma_{ii} \langle \hat{\sigma}_i^+ \hat{\sigma}_i^- \rangle(\tau) + \sum_{i \neq j=1}^N \gamma_{ij} \langle \hat{\sigma}_i^+ \hat{\sigma}_j^- \rangle(\tau), \quad (\text{A4})$$

where  $\langle \hat{\sigma}_i^+ \hat{\sigma}_j^- \rangle(\tau) \equiv \text{Tr}_A(\hat{\sigma}_i^+ \hat{\sigma}_j^- \hat{\rho}(\tau))$ , with  $\text{Tr}_A(\cdot)$  denoting the trace over atoms. For  $i \neq j$ ,  $\gamma_{ij}$  quantifies the influence of  $i$ th and  $j$ th atoms on each other's dynamics. For a one-dimensional array with interatomic spacing much larger than the transition wavelength of each atom, we have  $\gamma_{ij} = \gamma_0 \delta_{ij}$ , leading to an incoherent emission rate of  $\Gamma(\tau) = N\gamma_0 e^{-\gamma_0\tau}$ , where  $\gamma_0$  is the spontaneous emission rate of a single atom.

In order to obtain the two-point correlation function  $\langle \hat{\Phi}(\tilde{x}_i(\tau)) \hat{\Phi}(\tilde{x}_j(0)) \rangle$  of the field (required to compute the

transition rates and the cooperation  $\gamma_{ij}$ ), we need appropriate modes for quantization of the scalar field, which incorporate loss through boundaries in terms of reflection and transmission coefficients [39]. Note that we can evaluate the two-point correlator of the scalar field either by expanding the field in terms of the Rindler modes or by plugging the trajectory

$$t(\tau) = a^{-1} \sinh(a\tau), \quad z(\tau) = a^{-1} \cosh(a\tau) \quad (\text{A5})$$

of the Rindler atoms in the scalar field expanded in terms of the inertial modes. We take the latter route. To this end, next, we obtain the field modes inside a lossy planar cavity.

### Field Quantization Between Two Leaky Parallel Mirrors

Let us consider two infinite parallel mirrors P1 and P2 at  $x = -L/2$  and  $x = +L/2$  in Cartesian coordinates, forming a planar cavity. Unitarity of operation requires the complex reflection ( $r_1, r_2$ ) and transmission ( $t_1, t_2$ ) coefficients of the mirrors to satisfy [39]:

$$\begin{aligned} |r_1|^2 + |t_1|^2 &= |r_2|^2 + |t_2|^2 = 1, \\ r_1^* t_1 + r_1 t_1^* &= r_2^* t_2 + r_2 t_2^* = 0. \end{aligned} \quad (\text{A6})$$

As we are interested in spatial modes between mirrors,

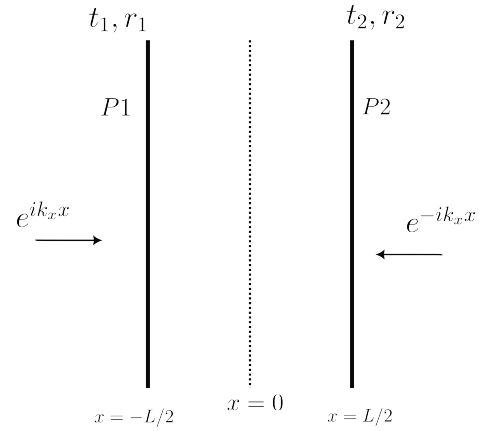


FIG. A1. Cross-sectional view of the planar cavity formed by two parallel mirrors with complex transmission and reflection coefficients  $t_i$  and  $r_i$ , respectively. The field modes between the mirrors are determined from the plane wave modes  $e^{\pm ik_x x}$  incident on the mirrors [39].

note that plane waves in  $\hat{x}$  direction incident on mirrors from left and right give rise to two distinct spatial mode profiles in between the mirrors depending upon reflection and transmission coefficients [40],

$$U_{k_x}(x) = \frac{1}{D} (t_1 e^{ik_x x} + t_1 r_2 e^{-ik_x x + ik_x L}) \quad \text{and} \quad (\text{A7})$$

$$U'_{k_x}(x) = \frac{1}{D} (t_2 e^{-ik_x x} + t_2 r_1 e^{ik_x x + ik_x L}), \quad (\text{A8})$$

where  $D = 1 - r_1 r_2 e^{2ik_x L}$  and  $k^2 = k_x^2 + k_y^2 + k_z^2$ . The creation and annihilation operators  $\hat{a}_k, \hat{a}_k^\dagger$  for  $U_{k_x}$ , and  $\hat{a}'_k, \hat{a}'_k{}^\dagger$  for  $U'_{k_x}$  satisfy the commutation relations  $[\hat{a}_k, \hat{a}'_{k'}] = [\hat{a}'_k, \hat{a}'_{k'}] = \delta(k - k')$ , and  $[\hat{a}_k, \hat{a}'_{k'}] = [\hat{a}'_k, \hat{a}_{k'}] = 0$ .

Following the standard quantization procedure, the quantized scalar field between two parallel mirrors, providing for the mirror imperfections through non-ideal reflectivities, can be expressed as:

$$\hat{\Phi}(\tilde{x}) = \int \frac{d^3 k}{(2\pi)^{3/2}} \frac{1}{\sqrt{2\omega_k}} (\hat{a}_k U_{k_x}(x) e^{-i\omega_k t + ik_y y + ik_z z} + \hat{a}'_k U'_{k_x}(x) e^{-i\omega_k t + ik_y y + ik_z z} + \text{h.c.}), \quad (\text{A9})$$

where  $\tilde{x} \equiv (t, x, y, z)$  now denotes a spacetime event expressed in the inertial coordinates. For symmetrical identical mirrors,  $t_1 = t_2 = i|t_1| = i|t_2| = i\mathcal{T}$  and

$r_1 = r_2 = -|r_1| = -|r_2| = -\mathcal{R}$ , the two-point function of the field,  $\mathcal{W}(\tilde{x}_i, \tilde{x}_j) = \langle \hat{\Phi}(\tilde{x}_i) \hat{\Phi}(\tilde{x}_j) \rangle$  can be computed to be:

$$\mathcal{W}(\tilde{x}_i, \tilde{x}_j) = \int \frac{d^3 k}{(2\pi)^3} \frac{1}{2\omega_k} e^{-i\omega_k(t_i - t_j)} \times e^{ik_y \Delta y_{ij} + ik_z \Delta z_{ij}} \frac{2\mathcal{T}^2}{|D|^2} \left\{ (1 + \mathcal{R}^2) \cos(k_x(x_i - x_j)) - 2\mathcal{R} \cos(k_x(x_i + x_j)) \cos(k_x L) \right\}. \quad (\text{A10})$$

### $\gamma_{ij}$ for a Rindler Array

Starting with Eq. (A3) and using field's expansion in terms of the inertial modes obtained in Eq. (A9), and plugging in the trajectory of a Rindler atom we obtain

$$\gamma_{ij}^{(a)} = \int_{-\infty}^{+\infty} ds e^{i\omega_0 s} \int \frac{d^2 k_\perp}{(2\pi)^3} \rho(k_x, L, \mathcal{R}) e^{ik_y(y_i - y_j)} \int_{-\infty}^{+\infty} \frac{dk_z}{\omega_k} \exp\left(-\frac{2i}{a} \sinh\left(\frac{as}{2}\right) [\omega_k \cosh(a\tilde{\tau}) - k_z \sinh(a\tilde{\tau})]\right), \quad (\text{A11})$$

where  $s \equiv \tau_i - \tau_j$  and  $\tilde{\tau} \equiv (\tau_i + \tau_j)/2$ . Transforming to new variables  $\omega'_k = \omega_k \cosh(a\tilde{\tau}) - k_z \sinh(a\tilde{\tau})$  and  $k'_z = k_z \cosh(a\tilde{\tau}) - \omega_k \sinh(a\tilde{\tau})$ , one obtains Eq. (2) of the main text. Further, for  $i = j$  and  $a \rightarrow 0$ , we obtain the spontaneous emission rate of an inertial atom inside a planar cavity. For higher values of the mirror reflectivity, the emission rate of an inertial atom in the sub-resonant cavity configuration is suppressed more strongly, as illustrated in Fig. A2.

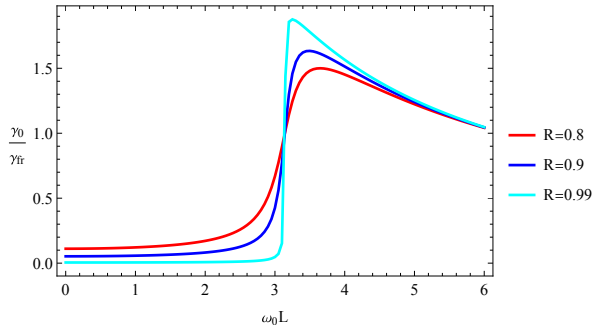


FIG. A2. Effect of cavity mirror reflectivity on spontaneous emission rate of a single inertial atom as a function of the separation between the mirrors.

### Coherent dipole-dipole interactions

The strength of the coherent dipole-dipole interactions in the atomic array is quantified by  $\Omega_{ij}$  (see Eq.(A2)). For Rindler and inertial atomic arrays inside the planar cavity, we obtain

$$\Omega_{ij}^{(a)} = - \int \frac{d^2 k_\perp}{(2\pi)^2} \rho(k_x L, \mathcal{R}) e^{ik_y y_{ij}} \frac{K_{i\omega_0/a}(k_\perp/a)}{a} \times (I_{-i\omega_0/a}(k_\perp/a) + I_{i\omega_0/a}(k_\perp/a)), \quad (\text{A12})$$

and

$$\Omega_{ij}^{(0)} = - \int \frac{d^2 k_\perp}{(2\pi)^2} \rho(k_x L, \mathcal{R}) e^{ik_y y_{ij}} \frac{\Theta(k_\perp - \omega_0)}{\sqrt{k_\perp^2 - \omega_0^2}}, \quad (\text{A13})$$

respectively, where  $I_{i\nu}(x)$  and  $K_{i\nu}(x)$  are the modified Bessel functions of first and second kind, respectively.

The field-mediated coherent dipole-dipole interactions between atoms in the array cause collective Lamb shift in each atom's energy levels [11, 41]. The total Lamb shift (including both individual and collective contributions) of the atom at the  $i$ th site is given as  $\Omega_i = \sum_{j=1}^N \Omega_{ij}$ . The inhomogeneity in the array introduced by the coherent dipole-dipole interactions, that causes dephasing of the atomic dipoles, is given by the variance of  $\Omega_i, i = 1, 2, \dots, N$ . The characteristic time scale over which dephasing occurs between a pair of atoms depends on the difference between the total phase acquired by the pair. To address the problem of dephasing, one effective



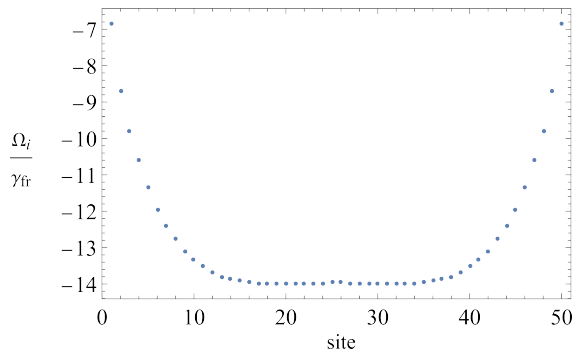


FIG. A3. The cooperative Lamb shift as a function of site in a Rindler atomic array containing fifty atoms. Atoms in the bulk of the array experience almost identical environments and hence suffer similar shifts. Therefore, dephasing due to coherent dipole-dipole interactions is reduced in such ordered arrangements. The plot is for  $a/\omega_0 = 10^{-5}$  and  $d/\lambda_0 = 1$ .

approach involves configuring the spatial arrangement of atoms so that each atom experiences a symmetric environment. A symmetric environment ensures uniformity in the phase accumulation, thereby minimizing the disparities in the phase acquired by different atoms. A sufficiently long ordered array fulfills this requirement, as atoms in the bulk experience almost identical environment and accumulate phase uniformly, ensuring dephasing effects are minimal.

For accelerations of interest, we confirm that this is also the case for a Rindler array. As shown in Fig. A3, the atoms in the bulk of an ordered array are shielded from this inhomogeneity as they experience an identical environment. Overall, for an appropriate choice of  $d/\lambda_0$ , the coherent dipole-dipole interactions between atoms cause only a slow dephasing even in an accelerated array. The atoms in the bulk thus remain indiscernible with respect to their coupling to the electromagnetic field, therefore, the evolution of these atoms proceeds in a permutationally invariant (under  $i \leftrightarrow j$ ) manner.

### Total Emission Rate

For the initial state of the array, we consider the product state

$$\hat{\rho}(0) = \prod_i |\theta_0, \varphi_0\rangle_i \langle \theta_0, \varphi_0|, \quad \theta_0 < \pi, \quad (\text{A14})$$

$$\Gamma(\tau) = \frac{\gamma_0(1 - \cos \theta_0)N(\mu N + 1)^2[(1 + \cos \theta_0)\mu N + 2]e^{\gamma_0\tau(\mu N + 1)}}{([\mu N(1 + \cos \theta_0) + 2]e^{\gamma_0\tau(\mu N + 1)} + (1 - \cos \theta_0)\mu N)^2}. \quad (\text{A18})$$

For  $\mu > 0$  and  $\theta_0 \rightarrow \pi$ , the above equation can be rear-

where

$$|\theta_0, \varphi_0\rangle_i = \sin(\theta_0/2)e^{-i\varphi_0/2}|e\rangle_i + \cos(\theta_0/2)e^{i\varphi_0/2}|g\rangle_i,$$

with  $|e\rangle_i$  and  $|g\rangle_i$  denoting the excited and ground states, respectively, of a two-level atom.

To obtain the total emission rate from Eq. (A4), we need  $\langle \sigma_i^+ \sigma_j^- \rangle(t)$ . In general, the two-particle mean values depend on three-particle mean values and so on [15, 42]. Thus, an exact solution of the problem requires solving an entire hierarchy of equations. Alternatively, one can resort to appropriate approximations to decouple the multi-particle mean values. Following [15, 42], we introduce the approximation  $\langle \sigma_i^z \sigma_j^z \rangle = \langle \sigma_i^z \rangle \langle \sigma_j^z \rangle$ , ( $i \neq j$ ) which introduces an inaccuracy of the order of  $1/N$ . Under this approximation, the total emission rate of the array is obtained as given in Eq. (1) as outlined below.

Note the identity

$$\sum_{i \neq j} \sigma_i^+ \sigma_j^- = \frac{1}{4} \sum_{i \neq j} (\vec{\sigma}_i \cdot \vec{\sigma}_j - \sigma_i^z \sigma_j^z), \quad (\text{A15})$$

where  $\vec{\sigma}_i \cdot \vec{\sigma}_j = \sigma_i^x \sigma_j^x + \sigma_i^y \sigma_j^y + \sigma_i^z \sigma_j^z$ ; and the fact that the permutation operator in terms of  $\vec{\sigma}$  is given by

$$P_{ij} = \frac{1}{2}(\mathbb{1} + \vec{\sigma}_i \cdot \vec{\sigma}_j). \quad (\text{A16})$$

As noted in the previous section, for atoms in the bulk of a long ordered array the evolution remains permutationally invariant, therefore  $\langle \sigma_i^z \rangle$  is the same for all such atoms and  $\langle P_{ij} \rangle = 1$  [15, 42]. Under these observations, one obtains [13, 15]

$$\Gamma(\tau) = -\frac{dW}{d\tau} = \gamma_0 \left[ \mu \left( \frac{N^2}{4} - W^2 \right) + \left( \frac{N}{2} + W \right) \right], \quad (\text{A17})$$

where  $W = \sum_k \langle \sigma_k^z \rangle / 2$  is the total (dimensionless) energy of the atomic system and we have defined  $\mu = (\gamma_0 N^2)^{-1} \sum_{i \neq j} \gamma_{ij}$ . Solving the differential equation with the initial condition  $W(0) = -N \cos \theta_0 / 2$ , we obtain

rearranged to obtain Eq. (1).